

Supporting Information

Table S1. Crystal data and structure refinements of $\text{Sn}_2(\text{SO}_4)_3$ determined from powder XRD data via Rietveld refinement^a

$M / \text{g mol}^{-1}$	525.56
Temperature / K	298(2)
Space group	$P\bar{1}$ (No. 2)
a / pm	484.95(1)
b / pm	811.45(1)
c / pm	1213.51(2)
$\alpha / {}^\circ$	88.987(2)
$\beta / {}^\circ$	86.438(2)
$\gamma / {}^\circ$	73.329(1)
Volume / 10^6 pm^3	456.57(1)
Z	2
$\rho_{\text{calcd}} / \text{g cm}^{-3}$	3.82
Radiation; wavelength $\lambda / \text{\AA}$	CuK α ; 1.54184
Diffractometer	Bruker D8 Advance
θ range / deg	2.5–40
Refined parameters	31
R_{Bragg}	0.004
R_p	0.005
R_{wp}	0.008
GooF	1.44

^a The respective standard deviations are given in parentheses.

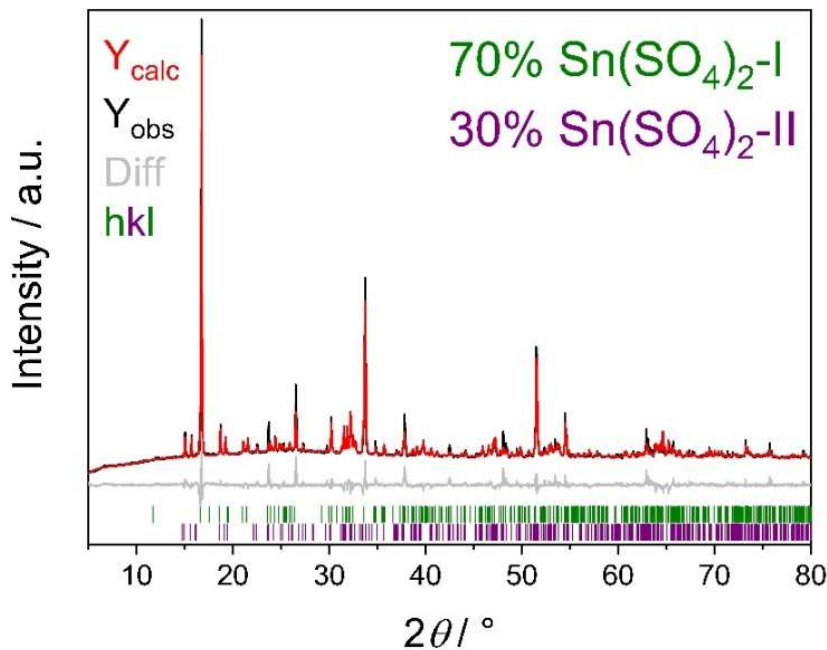


Fig. S1. Rietveld-Refinement of the mixed $\text{Sn}(\text{SO}_4)_2$ sample. Further details can be found in Tables S2.

Table S2. Crystal data and structure refinements on mixed $\text{Sn}(\text{SO}_4)_2$ determined from powder XRD data via Rietveld refinement^a

	$\text{Sn}(\text{SO}_4)_2\text{-I}$	$\text{Sn}(\text{SO}_4)_2\text{-II}$
$M / \text{g mol}^{-1}$	310.81	
Temperature / K	298(2)	298(2)
Space group	$P2_1/c$ (No. 14)	$P2_1/n$ (No. 14)
a / pm	504.27(4)	752.95(7)
b / pm	1065.53(7)	801.5(1)
c / pm	1065.76(7)	913.3(1)
$\beta / {}^\circ$	91.954(4)	92.533(4)
Volume / 10^6 pm^3	572.31(7)	550.6(1)
Z	4	
$\rho_{\text{calcd}} / \text{g cm}^{-3}$	3.61	3.75
Radiation; wavelength $\lambda / \text{\AA}$	CuK α ; 1.54184	
Diffractometer	Seifert 3003 TT	
θ range / deg	2.5–40	
Refined parameters	42	
R_{Bragg}	0.034	0.030
R_p	0.034	
R_{wp}	0.054	
GooF	0.40	

^a The respective standard deviations are given in parentheses.

Table S3. Crystal data and structure refinements on $\text{Sn}(\text{SO}_4)_2$ determined from powder XRD data via Rietveld refinement^a; the sample indicated by p was prepared via precipitation starting from tin in H_2SO_4 as a pale grey powder (see text under “thermal analysis” for further explanation)

	$\text{Sn}(\text{SO}_4)_2\text{-I}$	$\text{Sn}(\text{SO}_4)_2\text{-I}$	p- $\text{Sn}(\text{SO}_4)_2\text{-I}$
$M / \text{g mol}^{-1}$		310.81	
temperature / K	298(2)	673(2)	298(2)
space group	$P2_1/c$ (No. 14)	$P2_1/c$ (No. 14)	$P2_1/c$ (No. 14)
a / pm	504.68(2)	507.78(2)	502.29(1)
b / pm	1066.29(4)	1073.10(7)	1071.46(4)
c / pm	1066.46(6)	1071.18(8)	1070.53(4)
$\beta / {}^\circ$	91.945(4)	90.04(2)	90.138(3)
volume / 10^6 pm^3	573.57(4)	583.68(6)	576.14(3)
Z		4	
$\rho_{\text{calcd}} / \text{g cm}^{-3}$	3.60	3.54	3.58
radiation; wavelength $\lambda / \text{\AA}$		CuK α ; 1.54184	
diffractometer		Bruker D8 Advance	
θ range / deg	2.5–40	2.5–30	2.5–40
refined parameters	33	33	28
R_{Bragg}	0.019	0.026	0.017
R_p	0.016	0.03	0.009
R_{wp}	0.025	0.044	0.017
GooF	1.35	0.12	3.28

^a The respective standard deviations are given in parentheses.

Table S4. Crystal data and structure refinements of $\text{Sn}(\text{SO}_4)_2\text{-I}$, $\text{Sn}(\text{SO}_4)_2\text{-II}$ and $\text{Sn}_2(\text{SO}_4)_3$ determined from single crystal XRD; $\text{Sn}(\text{SO}_4)_2\text{-I}$ was refined as a two-component twin (HKLF 5)^a

	$\text{Sn}(\text{SO}_4)_2\text{-I}$	$\text{Sn}(\text{SO}_4)_2\text{-II}$	$\text{Sn}_2(\text{SO}_4)_3$
$M / \text{g mol}^{-1}$	310.81	310.81	525.56
crystal size / mm^3	$0.30 \times 0.18 \times 0.12$	$0.14 \times 0.07 \times 0.06$	$0.07 \times 0.04 \times 0.03$
temperature / K	200(2)	286(2)	250(2)
crystal system	monoclinic	monoclinic	triclinic
space group	$P2_1/c$ (No. 14)	$P2_1/n$ (No. 14)	$P\bar{1}$ (No. 2)
a / pm	504.34(3)	753.90(3)	483.78(9)
b / pm	1065.43(6)	802.39(3)	809.9(2)
c / pm	1065.47(6)	914.47(3)	1210.7(2)
$\alpha / {}^\circ$	90	90	89.007(7)
$\beta / {}^\circ$	91.991(2)	92.496(2)	86.381(7)
$\gamma / {}^\circ$	90	90	73.344(7)
volume / 10^6 pm^3	572.17(6)	552.66(4)	453.55(14)
Z	4	4	2
$\rho_{\text{calcd}} / \text{g cm}^{-3}$	3.61	3.74	3.85
absorption coefficient μ / mm^{-1}	5.2	5.4	6.3
$F(000) / e$	584	584	488
radiation; wavelength $\lambda / \text{\AA}$	$\text{MoK}\alpha$; 0.71073		
diffractometer	Bruker D8 Venture		
θ range / deg	2.704–39.997	3.379–42.496	2.625–24.992
absorption correction	Multi-scan		
transmission (min; max)	0.490; 0.749	0.415; 0.750	0.544; 0.752
index range $h k l$	$\pm 9 0 19 0 19$	$\pm 14 \pm 15 \pm 17$	$\pm 5 \pm 9 -12 14$
reflections collected	5940	41984	5982
independent reflections	4617	3970	1602
obs. reflections ($I > 2 \sigma(I)$)	3961	3585	1326
refined parameters	104	101	152
BASF	0.497(1)	-	-
R_{int}	0.019	0.041	0.052
R_1	0.050	0.021	0.048
R_2	0.096	0.033	0.0589
GooF	1.146	1.064	1.066
residual electron density (max; min) / $e^- \text{\AA}^{-3}$	2.77; -3.78	0.88; -0.64	0.78; -0.84

^a The respective standard deviations are given in parentheses.

Table S5. Wyckoff symbol, atomic coordinates x ; y ; z and equivalent isotropic displacement parameters U_{eq} and anisotropic displacement parameters U_{ij} in \AA^2 for $\text{Sn}(\text{SO}_4)_2\text{-I}^{\text{a}}$

Atom	Wyckoff symbol	x	y	z	U_{eq}	U_{11}	U_{22}	U_{33}	U_{23}	U_{13}	U_{12}
Sn1	2a	0	0	0	0.00310(6)	0.00284(11)	0.00311(11)	0.00334(11)	-0.00010(9)	0.00017(9)	-0.0001(1)
Sn2	2d	1/2	0	1/2	0.00301(6)	0.00280(11)	0.00233(10)	0.00390(11)	0.00006(9)	-0.00006(9)	-0.00001(10)
S1	4e	-0.5116(2)	-0.31152(8)	0.53181(8)	0.00412(13)	0.0032(3)	0.0026(3)	0.0065(3)	-0.0001(2)	-0.0005(3)	0.0002(3)
S2	4e	-0.0159(2)	0.04028(8)	0.30318(8)	0.00422(13)	0.0038(3)	0.0049(3)	0.0039(3)	-0.0003(2)	-0.0002(2)	-0.0005(3)
O11	4e	-0.4379(6)	-0.1864(3)	0.4810(3)	0.0081(5)	0.0089(11)	0.0018(10)	0.0137(12)	0.0003(9)	0.0009(9)	-0.0009(9)
O12	4e	-0.3325(6)	-0.3989(3)	0.4636(3)	0.0061(4)	0.0042(10)	0.0048(11)	0.0093(12)	-0.0016(9)	-0.0007(8)	0.0018(8)
O13	4e	-0.7842(5)	-0.3394(3)	0.4757(3)	0.0060(4)	0.0032(10)	0.0042(11)	0.0105(12)	0.0006(9)	-0.0016(8)	-0.0015(8)
O14	4e	-0.4974(6)	-0.3222(3)	0.6636(3)	0.0105(5)	0.0102(12)	0.0149(13)	0.0063(10)	0.0006(9)	-0.0018(10)	-0.0010(11)
O21	4e	0.0539(7)	0.1677(3)	0.2887(3)	0.0125(6)	0.0171(14)	0.0054(11)	0.0147(13)	0.0010(10)	-0.0019(11)	-0.0036(11)
O22	4e	-0.0030(6)	-0.0357(3)	0.1858(2)	0.0066(4)	0.0093(11)	0.0084(10)	0.0022(9)	0.0001(8)	-0.0006(9)	0.0002(10)
O23	4e	0.1565(6)	-0.0291(3)	0.3969(3)	0.0064(5)	0.0045(10)	0.0096(12)	0.0049(11)	0.0012(9)	-0.0024(8)	0.0000(8)
O24	4e	-0.2962(6)	0.0230(3)	0.3425(3)	0.0077(5)	0.0034(9)	0.0143(14)	0.0054(11)	0.0029(10)	0.0012(8)	0.0015(9)

^a The respective standard deviations are given in parentheses.

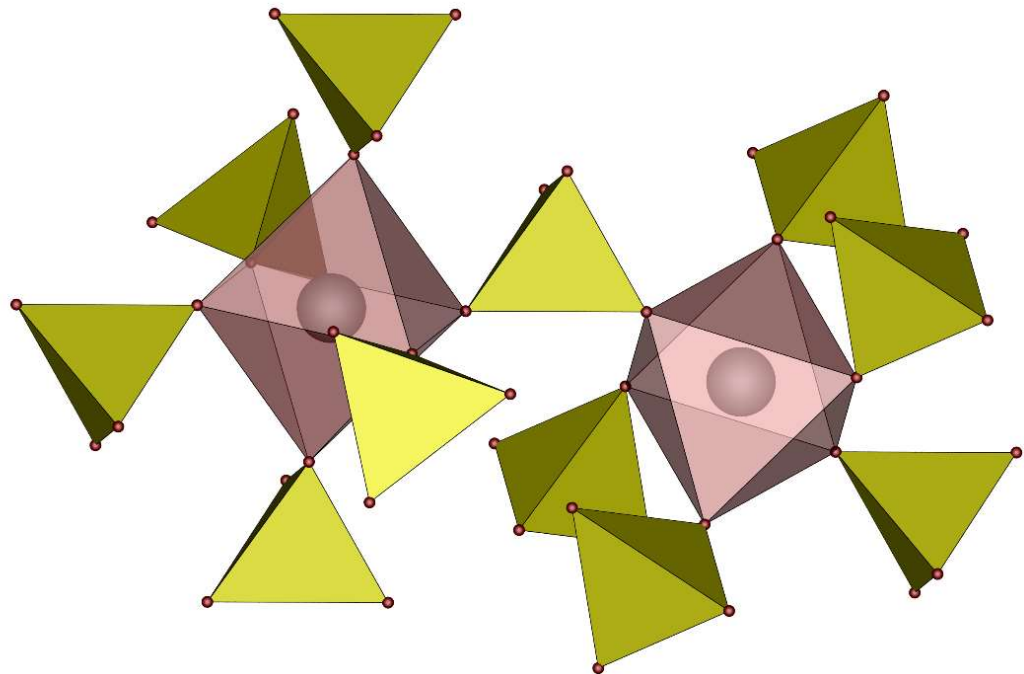


Fig. S2. Coordination environment and connection pattern of Sn^{4+} cations in $\text{Sn}(\text{SO}_4)_2\text{-I}$; Sn grey, O red, sulfate tetrahedra yellow, SnO_6 octahedra pale red.

Table S6. Selected interatomic distances (in pm) and angles (in °) in $\text{Sn}(\text{SO}_4)_2\text{-I}$ determined by single crystal XRD; the respective standard deviations are given in parentheses.

Distance / angle	
Sn-O	201.6(3)- 204.9(3)
$\Sigma \text{IR}(\text{Sn}-\text{O})^1$	204
S-O _c ^[a]	149.1(3)-150.9(3)
S-O _{nc} ^[a]	140.8(3)-141.2(3)
$\Sigma \text{IR}(\text{S}-\text{O})^1$	147
O-S-O	103.7(2)-115.5(2)

^[a] The S-O distances are discriminated between the ones containing oxygen atoms coordinating tin atoms O_c and the ones not coordinating tin atoms O_{nc}.

Table S7. Wyckoff symbol, atomic coordinates x ; y ; z and equivalent isotropic displacement parameters U_{eq} and anisotropic displacement parameters U_{ij} in Å² for Sn(SO₄)₂-II^a

Atom	Wyckoff symbol	x	y	z	U_{eq}	U_{11}	U_{22}	U_{33}	U_{23}	U_{13}	U_{12}
Sn1	4e	0.47634(2)	0.76560(2)	0.15989(2)	0.00520(2)	0.00515(2)	0.00540(3)	0.00507(3)	0.00013(2)	0.00042(2)	0.00017(2)
S1	4e	0.76125(3)	1.05382(3)	0.10574(3)	0.00623(4)	0.00579(8)	0.00636(9)	0.00642(9)	0.00056(7)	-0.00111(7)	-0.00068(6)
S2	4e	0.72985(3)	0.57594(3)	-0.07209(3)	0.00613(4)	0.00690(8)	0.00619(9)	0.00544(8)	0.00012(7)	0.00174(7)	-0.00057(7)
O11	4e	0.88289(12)	0.92022(11)	0.09936(10)	0.01330(14)	0.0114(3)	0.0108(3)	0.0177(4)	0.0013(3)	0.0003(3)	0.0045(3)
O12	4e	0.68727(11)	0.68732(11)	0.28692(9)	0.01020(13)	0.0096(3)	0.0108(3)	0.0099(3)	0.0020(2)	-0.0027(2)	0.0029(2)
O13	4e	0.26633(10)	0.85929(11)	0.03853(9)	0.00956(12)	0.0079(3)	0.0135(3)	0.0072(3)	0.0036(2)	-0.0006(2)	0.0002(2)
O14	4e	0.57957(10)	0.99847(10)	0.14989(9)	0.00903(12)	0.0076(3)	0.0079(3)	0.0116(3)	0.0006(2)	0.0005(2)	-0.0028(2)
O21	4e	0.81230(13)	0.49587(12)	0.05053(10)	0.01446(15)	0.0184(4)	0.0151(4)	0.0097(3)	0.0032(3)	-0.0016(3)	0.0035(3)
O22	4e	0.35148(12)	0.81921(12)	0.34519(9)	0.01241(14)	0.0138(3)	0.0140(4)	0.0099(3)	0.0009(3)	0.0057(3)	0.0068(3)
O23	4e	0.35188(12)	0.54300(11)	0.18232(9)	0.01158(13)	0.0172(3)	0.0087(3)	0.0087(3)	-0.0012(2)	0.0001(3)	-0.0051(3)
O24	4e	0.58148(11)	0.69057(12)	-0.03118(9)	0.01204(14)	0.0120(3)	0.0150(3)	0.0094(3)	-0.0017(3)	0.0032(2)	0.0050(3)

^a The respective standard deviations are given in parentheses.

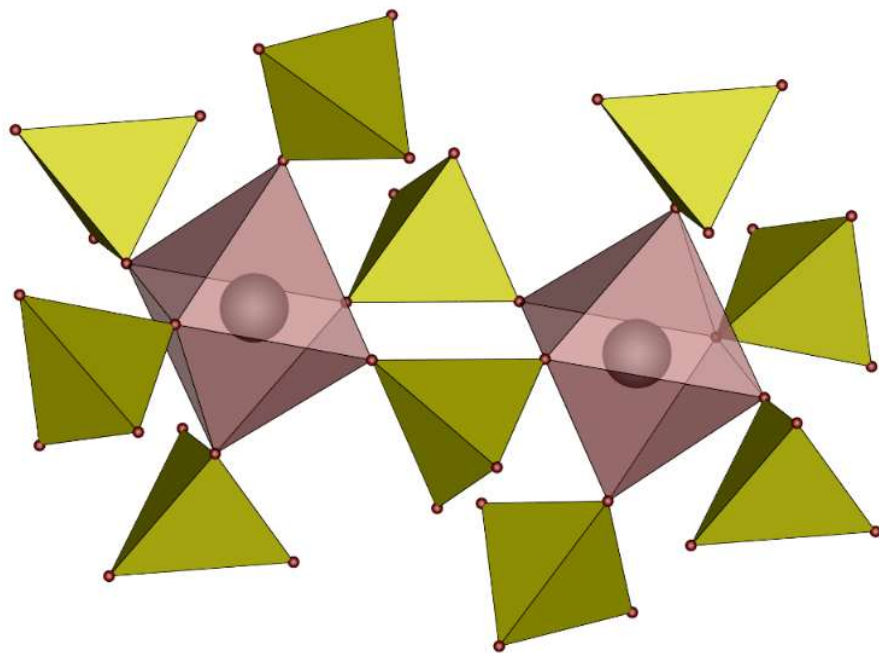


Fig. S3. Coordination environment and connection pattern of Sn^{4+} cations in $\text{Sn}(\text{SO}_4)_2\text{-II}$; Sn grey, O red, sulfate tetrahedra yellow, SnO_6 octahedra pale red.

Table S8. Selected interatomic distances (in pm) and angles (in °) in $\text{Sn}(\text{SO}_4)_2\text{-II}$ determined by single crystal XRD; the respective standard deviations are given in parentheses.

Distance / angle	
Sn-O	202.0(1)-204.1(1)
$\Sigma \text{IR}(\text{Sn}-\text{O})^1$	204
S-O _c ^[a]	147.7(1)-150.8(1)
S-O _{nc} ^[a]	141.3(1)-141.4(1)
$\Sigma \text{IR}(\text{S}-\text{O})^1$	147
O-S-O	104.35(5)-114.88(5)

^[a] The S-O distances are discriminated between the ones containing oxygen atoms coordinating tin atoms O_c and the ones not coordinating tin atoms O_{nc}.

Table S9. Wyckoff symbol, atomic coordinates x ; y ; z and equivalent isotropic displacement parameters U_{eq} and anisotropic displacement parameters U_{ij} in Å² for Sn₂(SO₄)₃^a

Atom	Wyckoff symbol	x	y	z	U_{eq}	U_{11}	U_{22}	U_{33}	U_{23}	U_{13}	U_{12}
Sn1	1a	0	0	0	0.00697(18)	0.0067(4)	0.0085(4)	0.0061(4)	0.0013(3)	-0.0014(3)	-0.0027(3)
Sn2	1b	0	0	1/2	0.00730(19)	0.0058(4)	0.0106(4)	0.0056(4)	-0.0005(3)	-0.0006(3)	-0.0024(3)
Sn3	2i	-0.19415(12)	-0.48742(7)	0.25400(4)	0.01624(17)	0.0163(3)	0.0155(3)	0.0188(3)	0.0020(2)	-0.0007(2)	-0.0078(3)
S1	2i	0.6315(4)	-0.2796(2)	0.54423(14)	0.0086(4)	0.0074(10)	0.0095(10)	0.0085(9)	0.0002(8)	-0.0018(7)	-0.0013(8)
S2	2i	0.3656(4)	0.2862(2)	0.01762(14)	0.0075(4)	0.0070(10)	0.0072(10)	0.0082(9)	0.0009(7)	-0.0006(7)	-0.0019(8)
S3	2i	0.1420(4)	-0.1553(2)	0.24885(14)	0.0078(4)	0.0099(10)	0.0110(10)	0.0037(8)	0.0014(7)	-0.0019(7)	-0.0045(8)
O11	2i	-0.2136(11)	-0.3611(6)	0.4457(4)	0.0140(12)	0.013(3)	0.016(3)	0.011(3)	-0.005(2)	0.005(2)	-0.001(2)
O12	2i	0.6778(11)	-0.3838(6)	0.6421(4)	0.0150(12)	0.012(3)	0.017(3)	0.017(3)	0.009(2)	-0.003(2)	-0.005(2)
O13	2i	0.2914(10)	0.1151(6)	0.4337(4)	0.0119(11)	0.009(3)	0.015(3)	0.014(3)	-0.005(2)	0.004(2)	-0.008(2)
O14	2i	0.3096(10)	-0.2231(6)	0.5289(4)	0.0101(11)	0.007(3)	0.004(3)	0.018(3)	0.002(2)	-0.006(2)	0.001(2)
O21	2i	0.2085(11)	-0.6561(7)	0.1201(4)	0.0212(13)	0.018(3)	0.030(4)	0.017(3)	-0.010(3)	0.006(2)	-0.010(3)
O22	2i	-0.3391(11)	-0.4145(6)	0.0666(4)	0.0156(13)	0.026(3)	0.012(3)	0.015(3)	0.010(2)	-0.012(2)	-0.014(3)
O23	2i	0.6806(10)	0.2157(6)	0.0403(4)	0.0106(8)	0.007(2)	0.008(2)	0.0162(19)	-0.0021(16)	-0.0033(15)	0.0002(16)
O24	2i	0.2802(10)	0.1379(6)	-0.0299(4)	0.0106(8)	0.007(2)	0.008(2)	0.0162(19)	-0.0021(16)	-0.0033(15)	0.0002(16)
O31	2i	-0.5588(11)	-0.2038(7)	0.2744(4)	0.0164(12)	0.010(3)	0.018(3)	0.018(3)	-0.002(2)	-0.004(2)	0.003(2)
O32	2i	0.0562(11)	-0.3023(6)	0.2110(4)	0.0132(12)	0.019(3)	0.014(3)	0.009(3)	-0.004(2)	0.000(2)	-0.009(2)
O33	2i	-0.0528(10)	-0.0735(6)	0.3455(4)	0.0117(11)	0.011(3)	0.021(3)	0.004(2)	-0.003(2)	0.001(2)	-0.007(2)
O34	2i	0.0886(11)	-0.0176(6)	0.1624(4)	0.0128(12)	0.025(3)	0.010(3)	0.006(3)	0.006(2)	-0.007(2)	-0.009(3)

^a The respective standard deviations are given in parentheses.

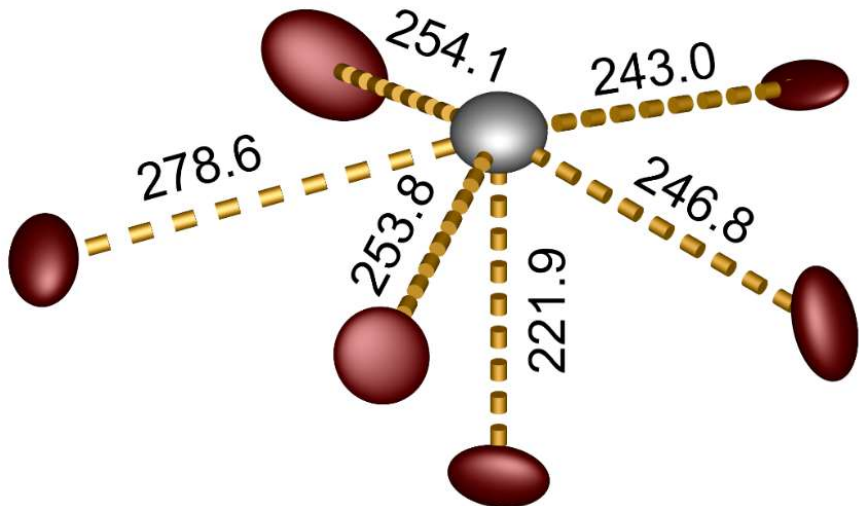


Fig. S4. $\text{Sn}(\text{II})\text{O}_6$ polyhedron in $\text{Sn}_2(\text{SO}_4)_3$: The respective bond lengths are given in pm; in the light of the VSEPR model the lone pair of the SnO_6E stereochemistry can be expected to point towards the top of this representation. Sn grey, O red, ellipsoids are shown at 80% probability.

Table S10. Selected interatomic distances (in pm) and angles (in $^\circ$) in $\text{Sn}_2(\text{SO}_4)_3$; the respective standard deviations are given in parentheses.

Distance / angle	
Sn(IV)-O	200.2(5)-203.1(5)
$\Sigma \text{IR}(\text{Sn(IV)-O})^1$	204
Sn(II)-O	221.8(5)-278.7(5)
$\Sigma \text{IR}(\text{Sn(II)-O})^2$	234.9
O-Sn(II)-O ^[a]	75.3(2)-82.3(2)
O-Sn(II)-O ^[b]	67.4(2)-76.2(2)
S-O	142.5(5)-151.5(5)
$\Sigma \text{IR}(\text{S-O})^1$	147
O-S-O	104.0(3)-115.4(3)

^[a]: angle in between the top and the base of the pentagonal pyramid; ^[b]: angle inside the base of the pentagonal pyramid.

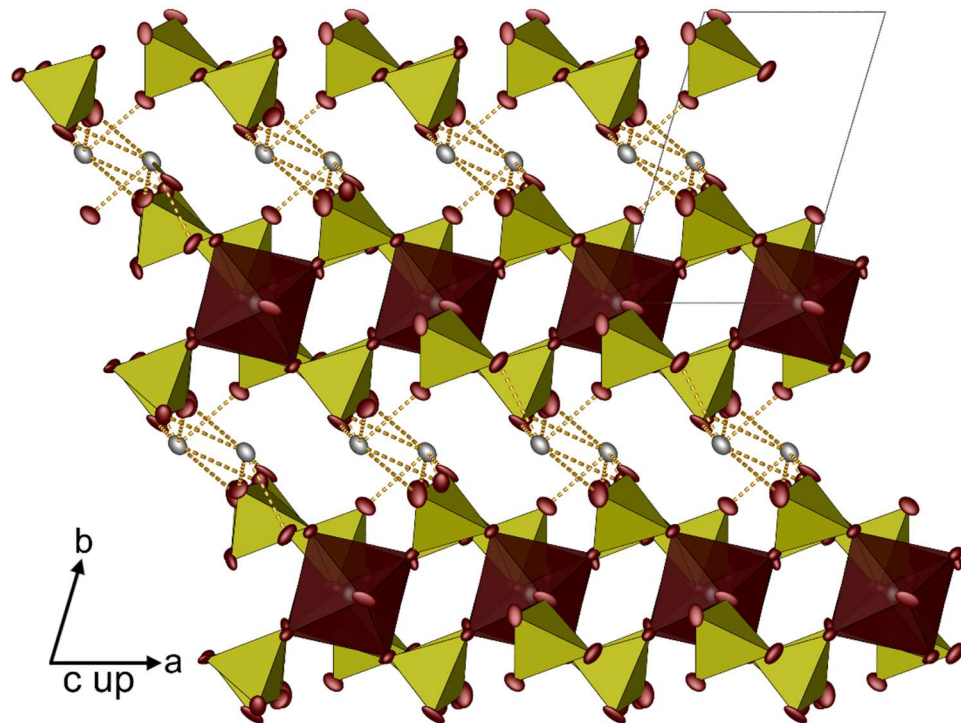


Fig. S5. Layered structure of $\text{Sn}_2(\text{SO}_4)_3$ viewed along (001); sulfate tetrahedra yellow, tin cations grey, oxygen atoms red, SnO_6 octahedra pale red; ellipsoids are shown at 80% probability.

Table S11. Electrostatic calculations for $\text{Sn}(\text{SO}_4)_2\text{-I}$, $\text{Sn}(\text{SO}_4)_2\text{-II}$ and $\text{Sn}_2(\text{SO}_4)_3$: the MAPLE values are compared to the sum of the MAPLE values of respective simple compounds; a deviation below 1% is our empirical benchmark for electrostatic consistency.

$\text{Sn}(\text{SO}_4)_2\text{-I}$	$\text{SnO}_2^3 + 2 \text{SO}_3^4$
MAPLE = 73337 kJ mol ⁻¹	MAPLE = 72873 kJ mol ⁻¹
	($\Delta = 0.6\%$)
$\text{Sn}(\text{SO}_4)_2\text{-II}$	$\text{SnO}_2^3 + 2 \text{SO}_3^4$
MAPLE = 73441 kJ mol ⁻¹	MAPLE = 72873 kJ mol ⁻¹
	($\Delta = 0.8\%$)
$\text{Sn}_2(\text{SO}_4)_3$	$\text{SnSO}_4^5 + \text{Sn}(\text{SO}_4)_2\text{-I}$
MAPLE = 108366 kJ mol ⁻¹	MAPLE = 107721 kJ mol ⁻¹
	($\Delta = 0.6\%$)

Table S12. ECon derived by MAPLE-calculations for Sn atoms in $\text{Sn}(\text{SO}_4)_2\text{-I}$

Atom	x	y	z	Distance / pm	Econ(1)	Econ(3)
Central atom						
Sn1	0	$\frac{1}{2}$	$\frac{1}{2}$			
Ligand						
O22	0.0027	0.5358	0.3141	201.719	1.028	1.028
O22	-0.0027	0.4642	0.6859	201.719	1.028	1.028
O12	-0.3324	0.3991	0.4637	201.757	1.027	1.027
O12	0.3324	0.6009	0.5363	201.757	1.027	1.027
O13	0.2158	0.3396	0.4758	204.72	0.940	0.940
O13	-0.2158	0.6604	0.5242	204.72	0.940	0.940
Next Ligand						
O21	-0.0539	0.3323	0.2111	356.134	0	0
Central atom						
Sn2	$\frac{1}{2}$	$\frac{1}{2}$	0			
Ligand						
O24	0.2965	0.477	0.1575	201.225	1.035	1.035
O24	0.7035	0.523	-0.1575	201.225	1.035	1.035
O11	0.5618	0.3138	-0.0191	201.954	1.013	1.013
O11	0.4382	0.6862	0.0191	201.954	1.013	1.013
O23	0.1567	0.4708	-0.1031	204.183	0.948	0.948
O23	0.8433	0.5292	0.1031	204.183	0.948	0.948
Next Ligand						
O23	-0.1567	0.5292	0.1031	353.916	0	0

Table S13. ECon derived by MAPLE-calculations for Sn atoms in $\text{Sn}(\text{SO}_4)_2\text{-II}$

Atom	x	y	z	Distance / pm	Econ(1)	Econ(3)
Central atom						
Sn1	0.4763	0.7656	0.1599			
Ligand						
O22	0.3515	0.8192	0.3453	202.052	1.031	1.031
O12	0.5796	0.9985	0.1499	202.768	1.010	1.010
O14	0.6873	0.6873	0.2869	202.782	1.009	1.009
O23	0.3519	0.543	0.1824	203.226	0.996	0.996
O13	0.2664	0.8593	0.0386	203.68	0.983	0.983
O24	0.5815	0.6905	-0.0313	204.138	0.969	0.969
Next Ligand						
O11	0.883	0.9202	0.0994	337.509	0	0

Table S14. ECon derived by MAPLE-calculations for Sn1 and Sn2 (Sn(IV) as well as Sn3 (Sn(II)) in $\text{Sn}_2(\text{SO}_4)_3$

Atom	x	y	z	Distance / pm	Econ(1)	Econ(4)
Central atom						
Sn1	0	0	0			
Ligand						
O24	-0.2802	-0.1379	0.0299	200.196	1.043	1.043
O24	0.2802	0.1379	-0.0299	200.196	1.043	1.043
O23	0.3194	-0.2157	-0.0403	201.605	1.001	1.001
O23	-0.3194	0.2157	0.0403	201.605	1.001	1.001
O34	-0.0886	0.0176	-0.1624	203.262	0.952	0.952
O34	0.0886	-0.0176	0.1624	203.262	0.952	0.952
Next Ligand						
O24	0.7198	-0.1379	0.0299	337.937	0	0
Atom	x	y	z	Distance / pm	Econ(1)	Econ(4)
Central atom						
Sn2	0	0	$\frac{1}{2}$			
Ligand						
O13	-0.2914	-0.1151	0.5663	202.119	1.014	1.014
O13	0.2914	0.1151	0.4337	202.119	1.014	1.014
O33	0.0528	0.0735	0.6545	202.597	1.000	1.000
O33	-0.0528	-0.0735	0.3455	202.597	1.000	1.000
O14	-0.3096	0.2231	0.4711	203.063	0.986	0.986
O14	0.3096	-0.2231	0.5289	203.063	0.986	0.986
Next Ligand						
O13	0.7086	-0.1151	0.5663	342.848	0	0
Atom	x	y	z	Distance / pm	Econ(1)	Econ(4)
Central atom						
Sn3	0.8058	0.5126	0.2540			
Ligand						
O32	1.0562	0.6977	0.2110	221.812	1.424	1.530
O22	0.6609	0.5855	0.0666	243.006	0.889	1.006
O31	0.4412	0.7962	0.2744	246.803	0.797	0.913
O21	1.2085	0.3439	0.1201	253.800	0.637	0.748
O11	0.7864	0.6389	0.4457	253.805	0.637	0.748
O12	1.3222	0.3838	0.3579	278.709	0.214	0.283
Next Ligand						
O12	0.3222	0.3838	0.3579	302.105	0.044	0.069

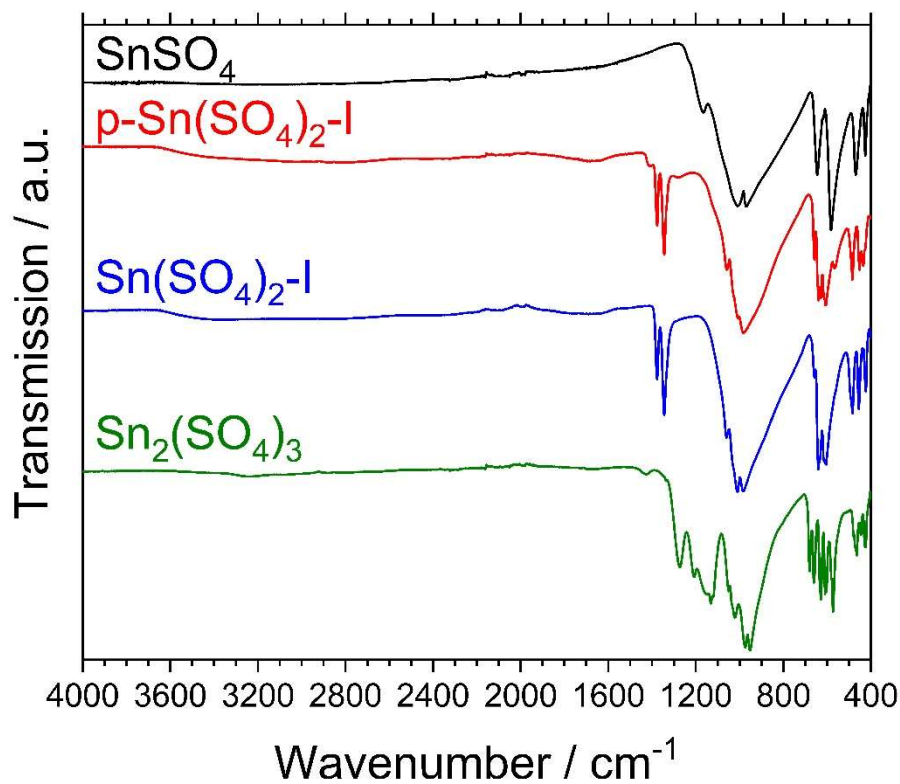


Fig. S6. Full FTIR spectra of SnSO_4 , $\text{Sn}(\text{SO}_4)_2\text{-I}$ and $\text{Sn}_2(\text{SO}_4)_3$ as well as $\text{Sn}(\text{SO}_4)_2\text{-I}$ prepared via precipitation ($\text{p-Sn}(\text{SO}_4)_2\text{-I}$)

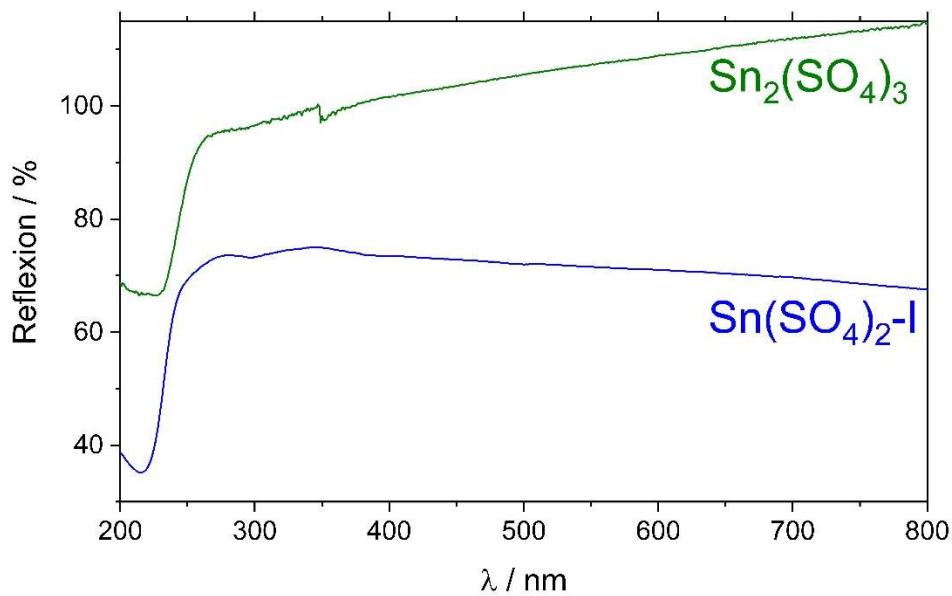


Fig. S7. Diffuse powder UV-vis spectra of $\text{Sn}(\text{SO}_4)_2\text{-I}$ and $\text{Sn}_2(\text{SO}_4)_3$: The artefact around 350 nm is due to lamp change during the measurement.

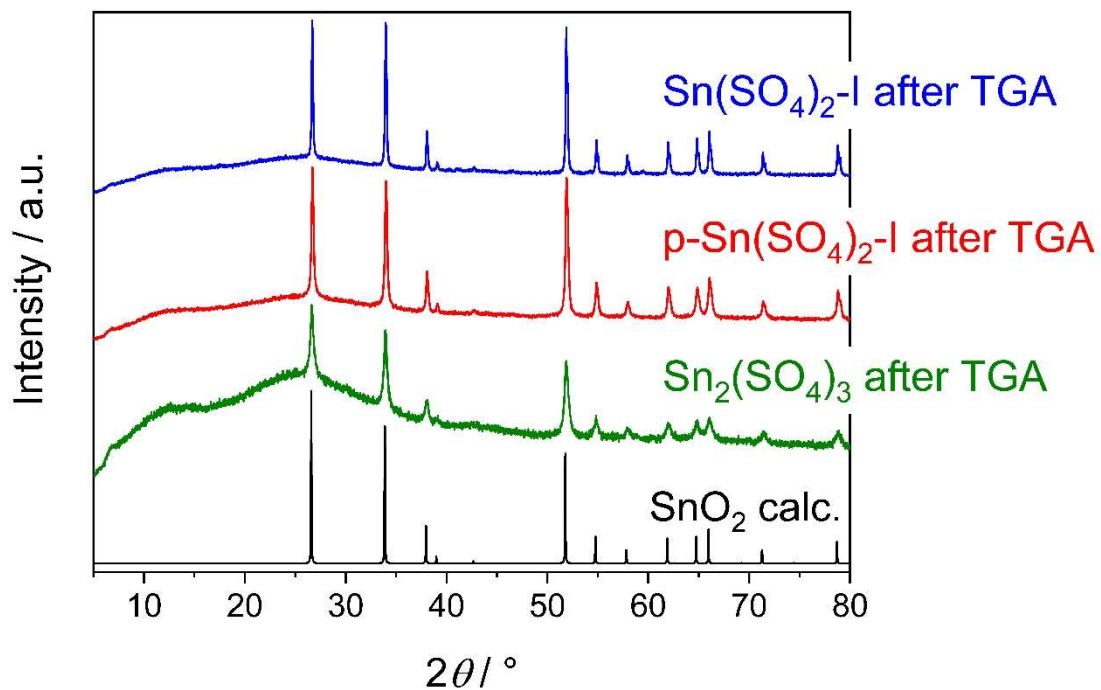


Fig. S8. Powder XRD patterns of the residues after the TGA measurements compared to a calculated pattern for SnO₂.³

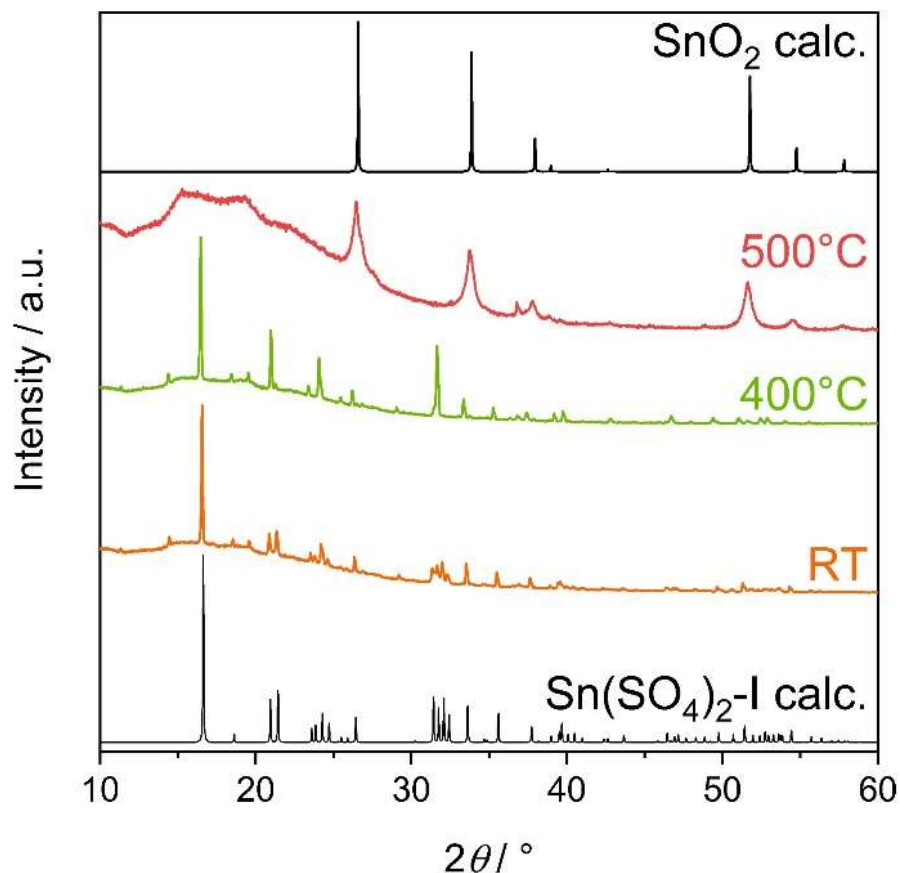


Fig. S9. TPXRD powder patterns of Sn(SO₄)₂-I compared to calculated patterns of Sn(SO₄)₂-I from our single-crystal XRD and SnO₂.³

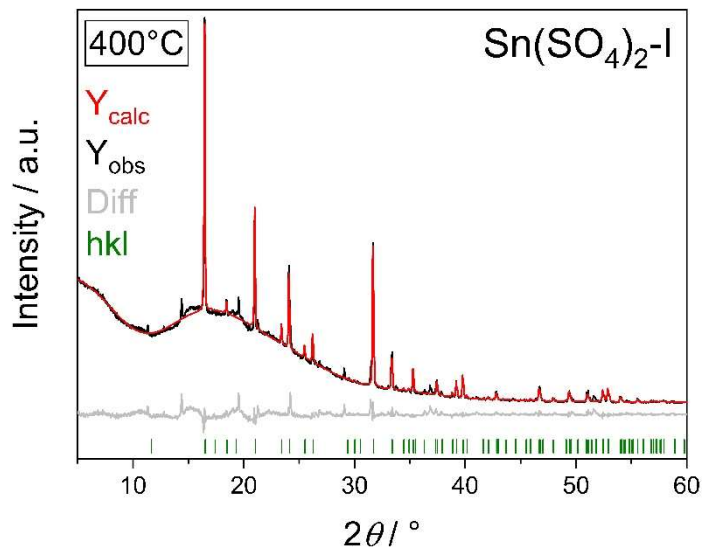


Fig. S10. Rietveld refinement on $\text{Sn}(\text{SO}_4)_2\text{-I}$ at 400°C . Further details can be found in Table S3.

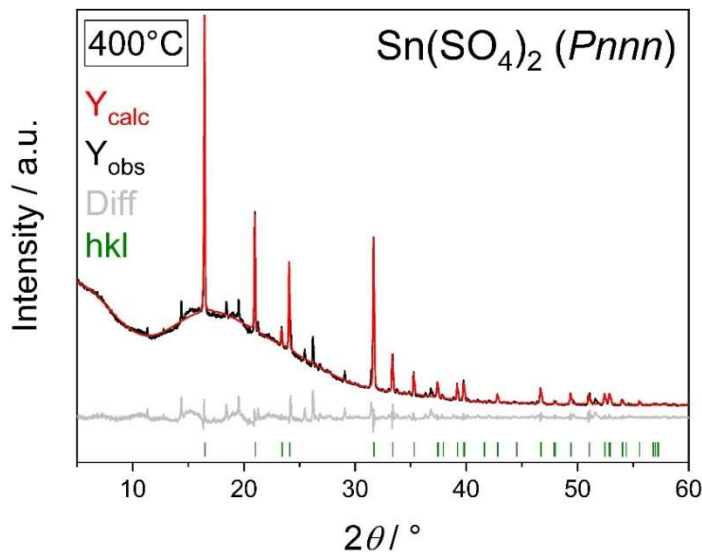


Fig. S11. Pawley fit on $\text{Sn}(\text{SO}_4)_2\text{-I}$ at 400°C . Further details can be found in the main text.

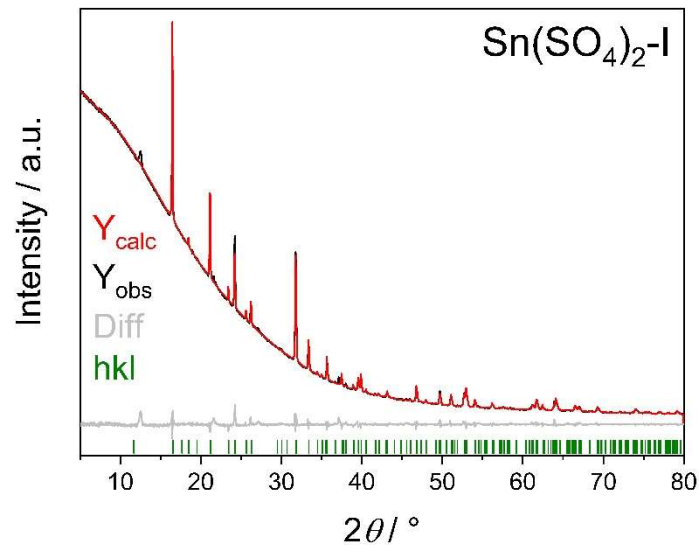


Fig. S12. Rietveld refinement on $\text{Sn}(\text{SO}_4)_2\text{-I}$ prepared by precipitation. Further details can be found in Table S3.

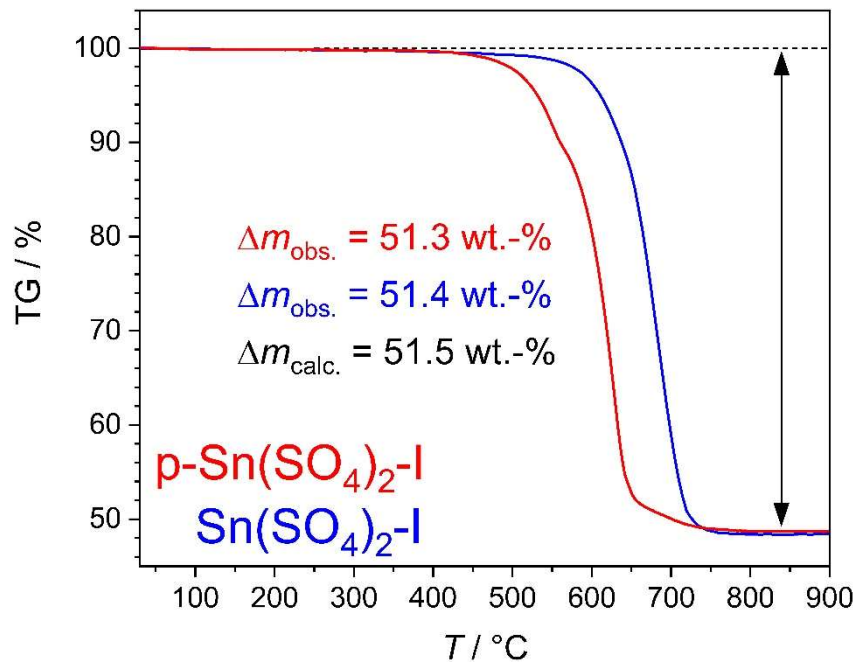


Fig. S13. Thermogravimetric analyses of $\text{Sn}(\text{SO}_4)_2\text{-I}$ and the $\text{Sn}(\text{SO}_4)_2\text{-I}$ sample prepared via precipitation (p- $\text{Sn}(\text{SO}_4)_2\text{-I}$)

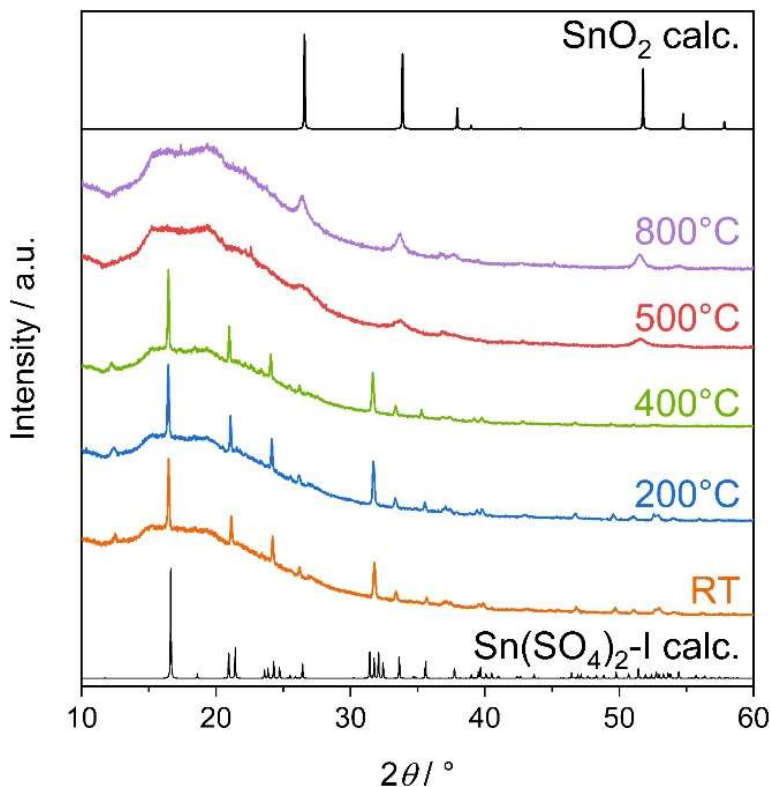


Fig. S14. TPXRD powder patterns of $\text{Sn}(\text{SO}_4)_2\text{-I}$ prepared via precipitation compared to calculated patterns of $\text{Sn}(\text{SO}_4)_2\text{-I}$ from our single-crystal XRD and SnO_2 .³

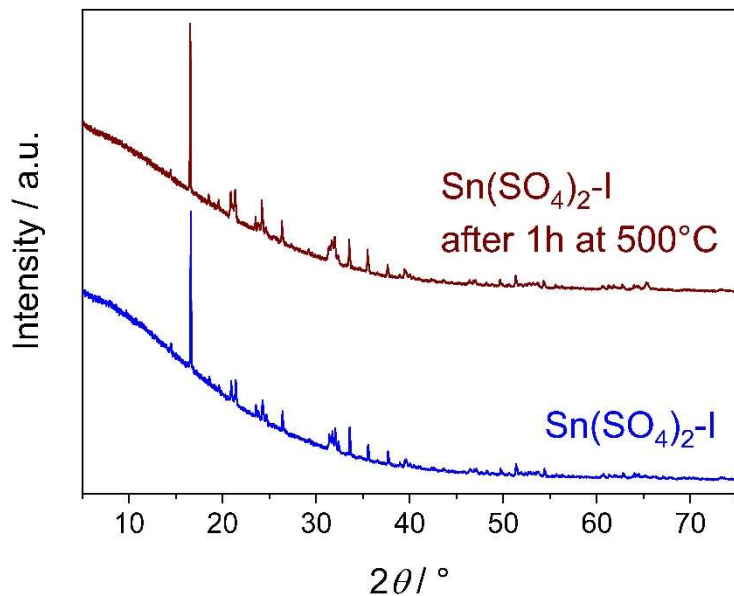


Fig. S15. Powder XRD patterns comparing as-prepared $\text{Sn}(\text{SO}_4)_2\text{-I}$ (bottom) and a sample heat treated at 500°C (top) showing almost no differences between both.

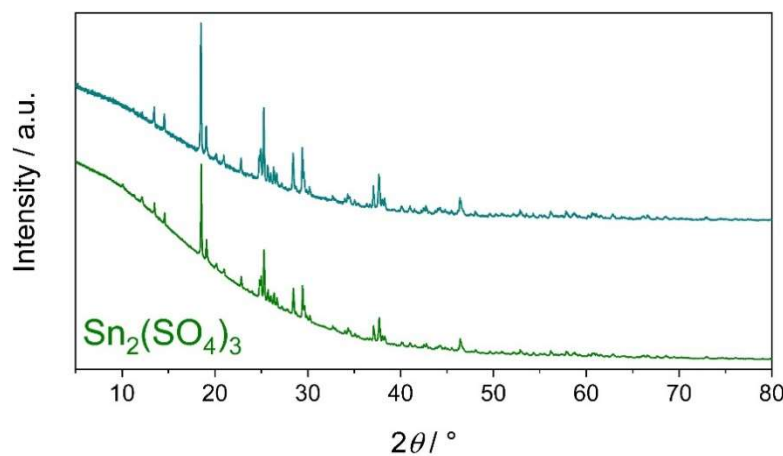


Fig. S16. Powder XRD patterns comparing as-prepared $\text{Sn}_2(\text{SO}_4)_3$ (bottom) and a sample heat treated at 450°C (top) showing almost no differences between both.

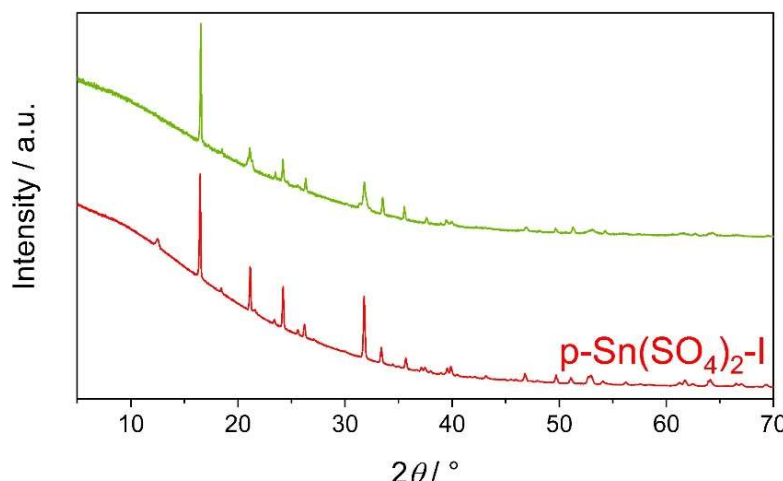


Fig. S17. Powder XRD patterns comparing as-prepared of as-prepared p- $\text{Sn}(\text{SO}_4)_2\text{-I}$ (bottom) and a $\text{Sn}_2(\text{SO}_4)_3$ sample heated at 300°C in air (top).

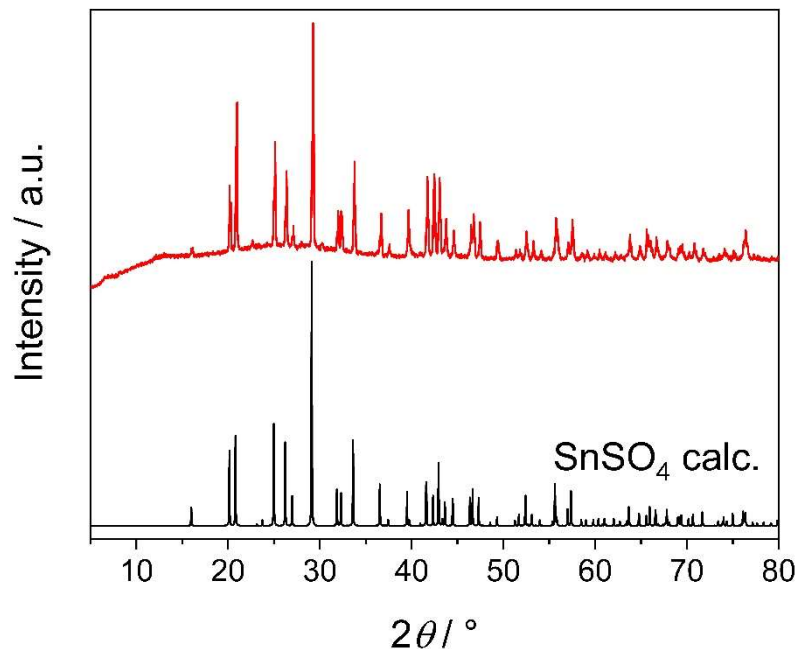


Fig. S18. Powder XRD pattern of as-prepared SnSO_4 compared to a calculated pattern.⁵

References

- 1 R. D. Shannon, *Acta Crystallogr. A*, 1976, **32**, 751–767.
- 2 A. A. B. Baloch, S. M. Alqahtani, F. Mumtaz, A. H. Muqabel, S. N. Rashkeev and F. H. Alharbi, *Phys. Rev. Mater.*, 2021, **5**, 1080.
- 3 W. H. Baur and A. A. Khan, *Acta Crystallogr. B*, 1971, **27**, 2133–2139.
- 4 R. Pascard and C. Pascard-Billy, *Acta Crystallogr.*, 1965, **18**, 830–834.
- 5 S. M. Antao, *Powder Diffr.*, 2012, **27**, 179–183.